Layer-by-Layer Immobilization of Gamma-Irradiated Polyacrylate-Stabilized Silver and Titanium Dioxide Nanocomposites

USMAN, Ken Aldren S.[1,a], TRINIDAD, Lawrence John Paulo L.[2,b] and PAYAWAN, Leon M. Jr.[1,2,c]

[1]Natural Sciences Research Institute, College of Science, University of the Philippines-Diliman, Quezon City, Philippines

[2]Institue of Chemistry, College of Science, University of the Philippines-Diliman, Quezon City, Philippines

[a]kenaldrenusman@yahoo.com, [b]ljptrinidad@gmail.com, [c]lmpayawan@yahoo.com

Keywords: Silver/poly(acrylic acid); TiO_2/poly(acrylic acid); Gamma irradiation; Layer-by-Layer Assembly; Surface Plasmon Resonance; Cyclic Voltammetry

Abstract. Layer-by-layer (L-b-L) assembly offers a simple, cost-efficient and portable technique in preparing inorganic thin films. However, preservation of the novel properties of such nanomaterials are the common issues raised regarding this method. In this study, γ-radiation reduced, silver/ poly(acrylic acid) (Ag/PAA) and TiO_2/ poly(acrylic acid) nanocomposites were deposited in glass substrate using L-b-L. Nanoparticle immobilization was done on different silica surfaces via layer-by-layer technique wherein the driving force for thin film formation is due to the electrostatic attraction between the negatively charged polymer shell and positive PDDA molecules. Characterization of the solution and bound form of the nanocomposites were done to evaluate the retention of their spectroscopic and electronic properties. The size distribution of the solution-phased nanocomposites were assessed using dynamic light scattering (DLS). The surface morphology, spectroscopic and electronic properties of the multilayer films were characterized using atomic force microscopy (AFM), scanning electron microscopy (SEM), UV-vis spectroscopy and cyclic voltammetry (CV).

Introduction

Interest for understanding behavioral properties of particles in the nano-sized range has surged in the past two decades. Advancements in the field include colloidal suspensions, microemulsions of single particles, nanotubes, nanowires, quantum dots as well as two- and three- dimensional assemblies. Particles at the nanometer range have energy levels that are not anymore band-like but discrete, owing to the *quantum size effect*. Nano-metal colloids manifest a unique property denoted as the surface Plasmon resonance observed in visible spectroscopy [4]. The excitation of the electrons in the confined electron gas and subsequent transition back to the unexcited state results in the plasma oscillation observed. The absorption maximum observed is dependent on size, dielectric property of the solvent, shape of the particles, proximity of the particles to one another, presence of adsorbates, and surface composition [5]. Properties such as these provide a way of quantifying nanoparticles and the extent of formation; however, to make them useful for advance materials, the task of generating and organizing with complete control must be overcome. Variance in size of the synthesized nanoparticles must be at minimum to avoid rigorous size classification procedures [6].

Several studies on immobilization of nanocomposites include encapsulation on beads, usage of metal-polymer matrix, etc. another technique used in organizing nanocomposites is via layer-by-layer (LbL) deposition. This method transfers a monolayer of surfactants that assembles unto a solid substrate, i.e. glass slide to form ultrathin stable films [1]. Electrostatic attractions are the main basis of the process. The negatively charged species adsorbed on silica surface subsequently adsorb a monoparticulate layer of positively charged colloidal particles from their dispersions, and a build-up of films can then be produced [1]. This simple, yet elegant technique allows the manipulation and engineering of charged molecular materials from solutions into 2D and 3D assemblies.

The retention of the plasmon resonance and electronic property after layer-by-layer immobilization could serve as a probe information of layers. The objective was to immobilize nanocomposites of Ag/Poly(acrylic acid) (Ag/PAA) and TiO_2/Poly(acrylic acid) (TiO_2/PAA) on glass surface using layer-by-layer technique with the polycation poly(diallyldimethylammonium chloride) (PDDA). Particle size distribution in solution was characterized using Zetasizer Photon Correlation Spectroscopy. Multilayer films of the nanocomposites were characterized using Scanning electron Microscopy (SEM), Atomic force microscopy (AFM), Surface Plasmon Resonance (SPR) and Cyclic voltammetry (CV).

Experimental

Synthesis of nanocomposites

Polymer-encapsulated silver and titania were generated from γ-irradiation of their aqueous solutions wiith poly(acrylic acid) (450 KDa) as stabilizer. Drop-wise additions of 2.0×10^{-3} M $AgNO_3$ to 15 mL PAA solutions, maintained at pH=8.5 were done in an inert atmosphere followed by addition of 2-propanol which served as a radical scavenger in the mixture. Similarly, drop-wise additions of 4000 ppm titania solution to separate 2000 ppm PAA solutions, maintained at pH=4.5 were done. Solutions were irradiated using Cobalt-60 Gamma cell 220 with a dose rate of 3.3 kGy/hr and a total dose of ~15kGy.

Layer-by-layer assembly

Cleaned microscope glass slides (VWR International), quartz slides (Ted Pella) and Indium Tin Oxide slides (Sigma Aldrich) were cut into 1.25 cm x 4.5 cm sizes and 1cm x 2cm sizes, respectively. Slides were dipped in a coating solution for 15 minutes, beginning with a layer of PDDA, and followed by rinsing with deionized water and by drying with a stream of Nitrogen gas. Slides were then dipped in the nanocomposite solution to complete the one layer consisting the polycation PDDA and polyanion layers, denoted as $(PDDA:C)_n$ where n is the number of complete dipping cycles and C is the polyanion nanocomposite shell (Metal/PAA).

Characterization

Double-beam UV-Vis Spectrophotometer (Shimadzu) was used to analyze absorbance of nanocomposite solutions and multilayer assemblies on silica surfaces. Zetasizer Nano-ZS90 was used to obtain the average particle diameter of 1-mL sample. The SEM images were examined using S3400N-SEM (Hitachi) and Field Emission-SEM (Philips) while surface morphology was obtained by using Solver Pro Atomic Force Microscope (AFM) (NT-MDT). Cyclic voltammetry was performed using a CompactStat Ivium potentiostat.

Results and Discussions

Synthesis of Ag/PAA Nanocomposites

Addition of the silver salt to the PAA aqueous solution caused the expanded coil of the polymer to collapse into globular state through the interaction of carboxylate group with silver cations.

This allows the negatively charged polymer to form a spherical shell around the positive silver cations through electrostatic interaction [17]. The reduction of silver ion was done by using γ-rays emitted from Cobalt-60. This would result to the formation of PAA encapsulated Ag particle as shown by the scheme in Figure 1.

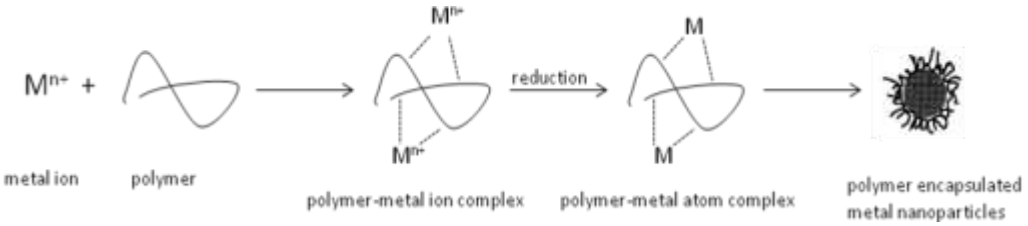

Figure 1. Schematic illustration of the process for the polymer protected metal nanoparticles.

Solutions of Ag/PAA solution turned yellowish to reddish brown with different color intensities upon exposure to γ-radiation. The varying color intensity of the solutions, manifested by their UV-Vis spectra, was found out to be a consequence of the varying molecular weight of the polymer used. Resulting UV-vis spectra in Figure 2 shows the characteristic Plasmon band of the

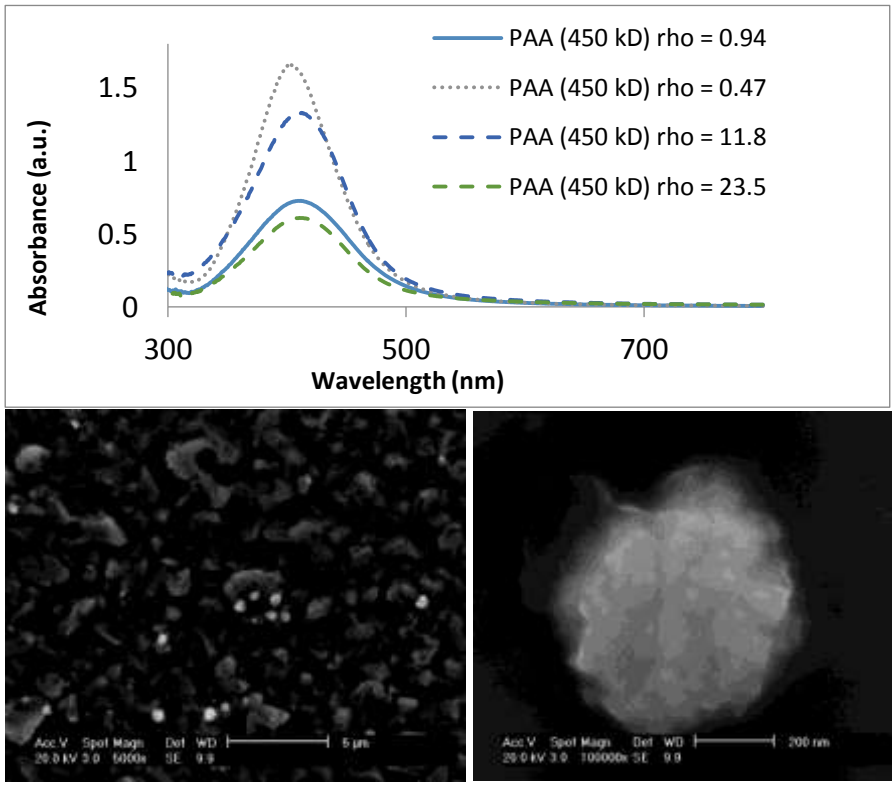

synthesized Ag/PAA nanocomposites at around 400nm.

Figure 2. *(Top)* UV-Vis spectra showing resulting plasmon bands of the irradiated samples selected from different sets of solutions. *(Bottom)* Scanning electron micrograph of Ag/PAA(ρ= 0.47)

The irradiation of silver ion in the absence of air and in the presence of a polymer leads to the display of the well-known Mie resonance around 400 nm [12]. The wavelength of maximum absorption is strongly dependent on the chemical modifications of the surface which results to an increase of the Fermi level due to a large electron charge density [12]. Concentration ratio of the silver salt to polymer was also found to considerably influence the shape and intensity of the surface plasmon band of the resulting Ag/PAA nanocomposites. For this discussion, the concentration ratio of polymer to silver salt in mg/ml is termed as rho, ρ. High ρ resulted to less intense surface plasmon bands, as compared to those with smaller ρ. This was attributed to the presence of excess $AgNO_3$ in the solution, which exhibits no Surface Plasmon even after irradiation [17]. The optimum ρ was 0.47 containing the most intense and symmetrical peak at 400 nm. Nevertheless, no shift in the wavelength of maximum absorbance occurred despite varying the MW and the salt: polymer ratio of the solutions.

Along the process, γ-radiation produced hydroxyl radicals from the cleavage of water molecules. These species react with the Ag, which could lead to the oxidation of the metal. Addition of 2-propanol to the solution of $AgNO_3$ and PAA provides secondary carbon radical scavengers that reacts with the hydroxyl radicals. Without the addition of 2-propanol, Ag/PAA solutions turned bluish-green with different color intensities after irradiation. UV-Vis spectra of solution prepared without 2-propanol exhibited absorption maxima at 600 nm as shown in Figure 3.

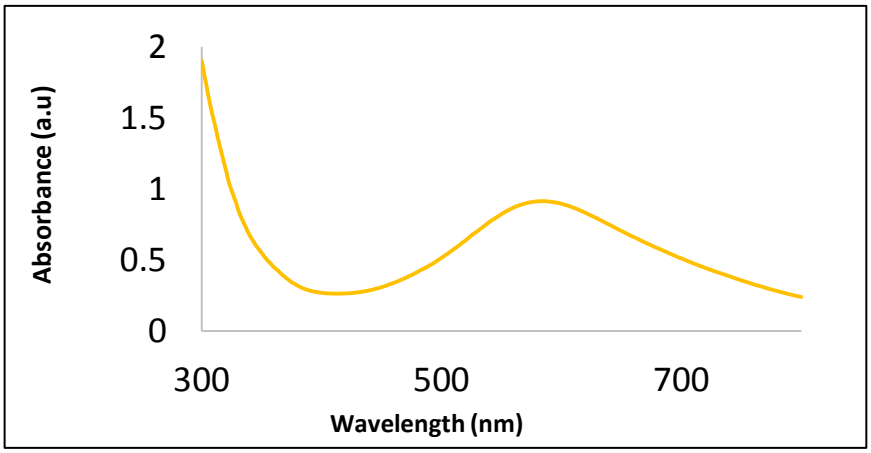

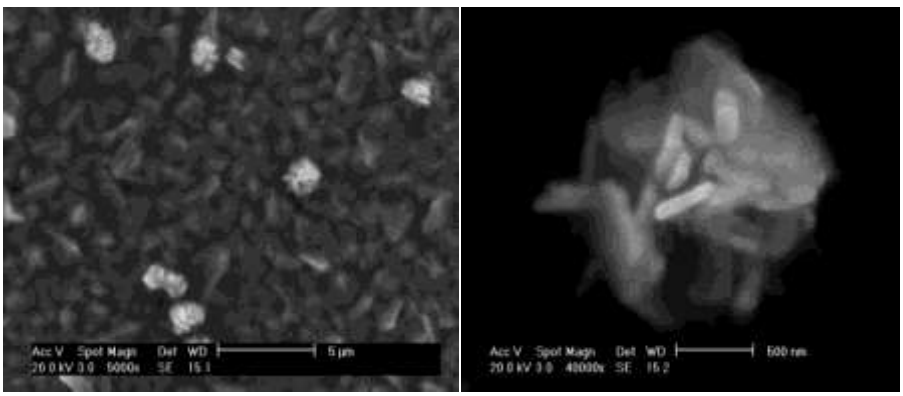

Figure 3. *(Top)* UV-vis spectra showing resulting Surface Plasmon Band of Ag/PAA (ρ= 0.47) without 2-propanol, *(Bottom)* Scanning electron micrograph of Ag/PAA (ρ= 0.47) without 2-propanol

The oxidation of the silver nanoparticles results to a red-shift of the plasmon resonance band. In this case, a red-shift of the absorbance to the 600 nm region can be attributed to the formation of Ag_7^{3+} species upon incomplete reduction of the Ag^+ ions due to the absence of 2-propanol [12]. The difference in the appearance of the nanocomposites, with and without addition of the radical scavenger, was also visible with the use of Scanning Electron Microscopy, shown by the images in Figure 3 *(right)*. The average size of the nanocomposite solutions were also analyzed, through Dynamic Light Scattering shown in Figure 4.

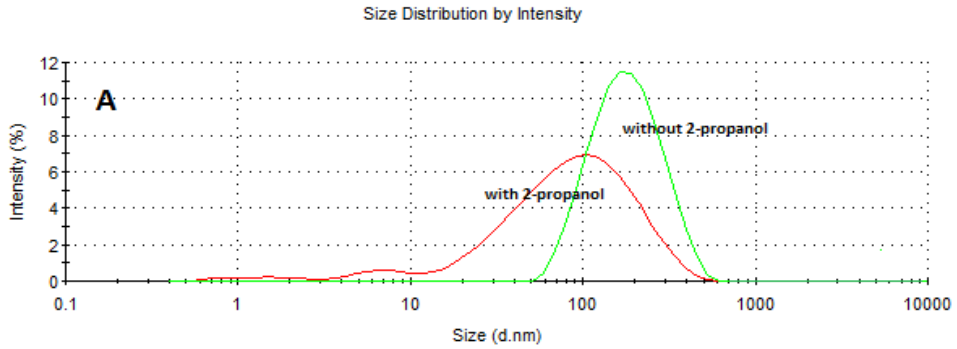

Figure 4. Dynamic Light Scattering Histogram of Ag/PAA (with and without 2-propanol)

Ag/PAA nanocomposites prepared in the presence of 2-propanol formed semi-spherical particles (Figure 2), otherwise clusters of rod-like structures would be formed (Figure 3). In addition, aggregation was also prominent for samples without 2-propanol wherein they formed large clusters. This was shown by the SEM image of the dried nanocomposites and DLS histogram of the colloidal solutions. Deposited nanocomposites revealed that globular clusters measuring around 500 nm in diameter were formed for samples with 2-propanol, while larger clusters measuring up to 1 μm were formed for the samples without 2-propanol. DLS profile of the solutions confirmed that addition of the radical scavenger produced smaller particles with average diameter of 59.88 nm compare to the 160.6 nm the sample without 2-propanol. Increase in their respective sizes were also attributed to the oxidation of the metal which gave way to the formation of clusters.

Synthesis of TiO_2/PAA Nanocomposites

Ratio of the concentrations of the metal and polymer greatly affect the size and the distribution of the metal-polymer nanocomposites in solution. An excess in one of the components would result in agglomeration of the particles and consequent precipitation.

Before irradiation, blob-like particulates were already visibly seen at the bottom of the 5:1 TiO_2:PAA solution indicating that a great excess in one of the components. After irradiating, the 5:1 and 2:1 solutions showed fine-grained particulates settling while that of the 1:3 TiO_2:PAA solution have silk-like precipitates. On the other hand, for the 1:1 and the 1:2 solutions only very minute fine and thread-like precipitates were observed. Separation of the

precipitates was done via decantation and the intensity of the bluish coloration increased in the series: 5:1 < 2:1 < 1:3 < 1:1 ≅1:2. The color originates from the colloidal TiO_2/PAA in solution, the clearer the solution, the less dissolved TiO_2/PAA; while the intense color signifies a greater amount of TiO_2/PAA.

UV-Vis spectroscopy of the solutions showed no significant peaks from 450-700 nm while a shoulder forms from 400 nm until a series of intense peaks in the far UV region starting at about 300 nm. The bands observed in the previous section were masked with the shoulder formation and thus characterization of particle absorption cannot be established through photometric methods. However, spectral scan for the solutions were done and shown in Appendix A. No significant differences in the spectra of the solutions were observed except for the spectra of the 5:1 TiO_2:PAA solution since high-energy charge transfer bands were absent in its spectrum. Absence of the said peaks implies that no absorbing species are present in solution; in other words, no or minute amount of TiO_2 and TiO_2/PAA are dissolved in 5:1 TiO_2:PAA solution. However, the absence of a descriptive peak wavelength that may be used for photometric studies have disabled the determination of the exact quantifiable ratio at which the amount of TiO_2 and PAA are optimum for the formation of uniformly sized particles.

SEM imaging of the 2:1, 1:1 and 1:2 solutions were done to observe the morphology and particle distribution. Aggregation of the particles was observed for the 2:1 and 1:1 solutions. Sharped-edge pebbles were prominent for these solutions. However, a closer examination of these pebbles show highly adsorbed spherical strictures of sizes ranging from about 40-120 nm depending on the ratio of solution as seen in Figure 2.b. EDX analysis shows that the sphere composition contains high amount of C and O, as well as about 10% Ti confirming these pimples were encapsulated TiO_2 nanometal produced.

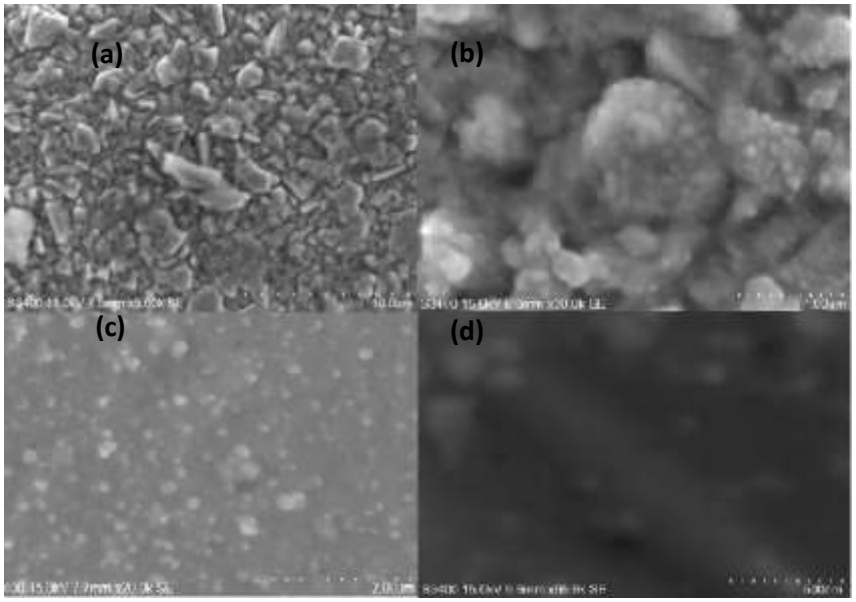

Figure 5. SEM images from (a) 2:1 TiO_2:PAA with 5,000x magnification, (b) 1:1 TiO_2:PAA and (c) 1:2 TiO_2:PAA with 20,000x magnification and (d) 2:1 TiO_2:PAA with 85,000x magnification in Copper TEM grids

Adsorption of the nanocomposites unto the excess metal explains the absence of TiO_2 peaks for the 5:1 TiO_2:PAA solution observed in the UV-Vis spectral scan. The non-encapsulated metal first aggregates, then becomes sites of nucleation of the negatively surface charged TiO_2/PAA nanocomposites since the bulk metal surface consist of positive charges as explained in Table 3 and attracts the negatively charged surface of the polymer cage of the nanocomposites.

Examination of the particle distribution by comparing the average inter-particle spacing revealed that 1:2 TiO_2:PAA solution has the most dispersed particles. For the 2:1 and 1:1 solutions, the nanocomposites are concentrated on the surfaces of the aggregated bulk titania. However, the 1:2 ratio has almost uniformly spaced nanocomposites with mono-nanocomposite sizes of about 60 to 80 nm. On the other hand, conjugated nanocomposites has also been observed consisting of 3 to 5 spheres, as shown in the encircled portion in Figure 5.c., of nanocomposites resulting to an increase in particle size. Despite the poor particle distribution of the 2:1 and 1:1 solutions, dispersed nanocomposites were still found in the area with low excess titania deposits as seen in Figure 5.d.

Layer-by-layer assembly of nanocomposite thin films

Immersion of the cleaned glass in a solution of the positive polyelectrolyte (PDDA) allowed adsorption of the first layer via electrostatic interaction of the polycation with the glass surface. Washing was done to remove loosely adsorbed PDDA and prevent contamination of the next solution. After drying, immersion in a solution of the nanocomposite allowed adsorption of the negatively surface charged-nanocomposite through electrostatic attraction, thus completing a single layer (n =1). This procedure was repeated as many times as necessary to achieve multiple layers of PDDA and nanocomposite on the glass substrate. The number of layers was monitored as a function of the intensity of plasmon bands exhibited by the nanocomposite deposited on glass.

UV absorbance

Plasmon bands of silver (400 nm) were retained even after deposition of the nanocomposites. Furthermore, the intensities of the bands were observed to increase with increasing number of layers as shown in Figure 6.

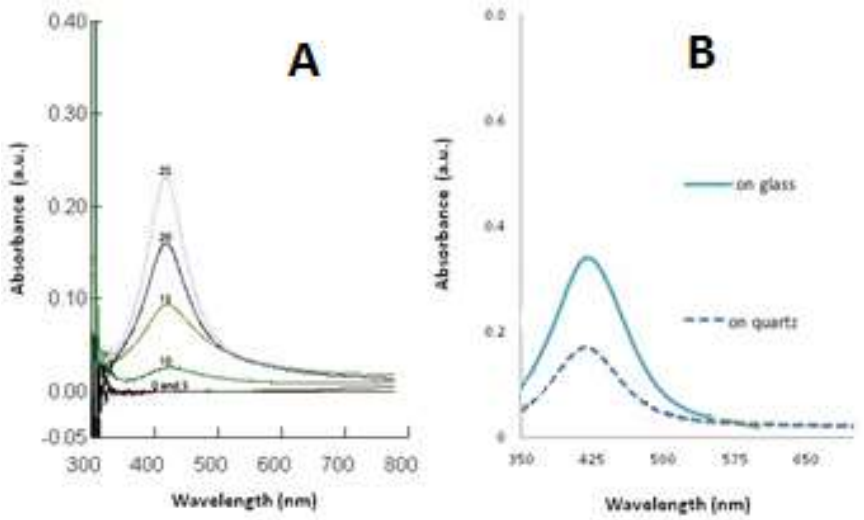

Figure 6. A. Surface plasmon band of (PDDA:Ag/PAA)$_n$ multilayer film where n is the number of layers (5, 10, 15, 20, and 25); (B) plasmon bands for 25 layers of Ag/PAA/PDDA on glass slide (indicated as line) and quartz slide (dash).

Both glass surfaces also showed the same wavelength of absorption. However, variation in substrate resulted to different intensities. Ordinary glass slide made from soda-lime-silica showed higher absorbance than those with pure silica quartz slide. This is due to the presence of sodium oxides and other impurities present in ordinary glass that increased the absorbance of light unlike those with quartz slide that contain pure and ordered crystalline silica structure.

On the other hand, the spectra of the TiO_2/PAA nanocomposites didn't show any maximum peak, which made it impossible to monitor the effect of increasing film thickness using UV-Vis spectroscopy.

Surface morphology

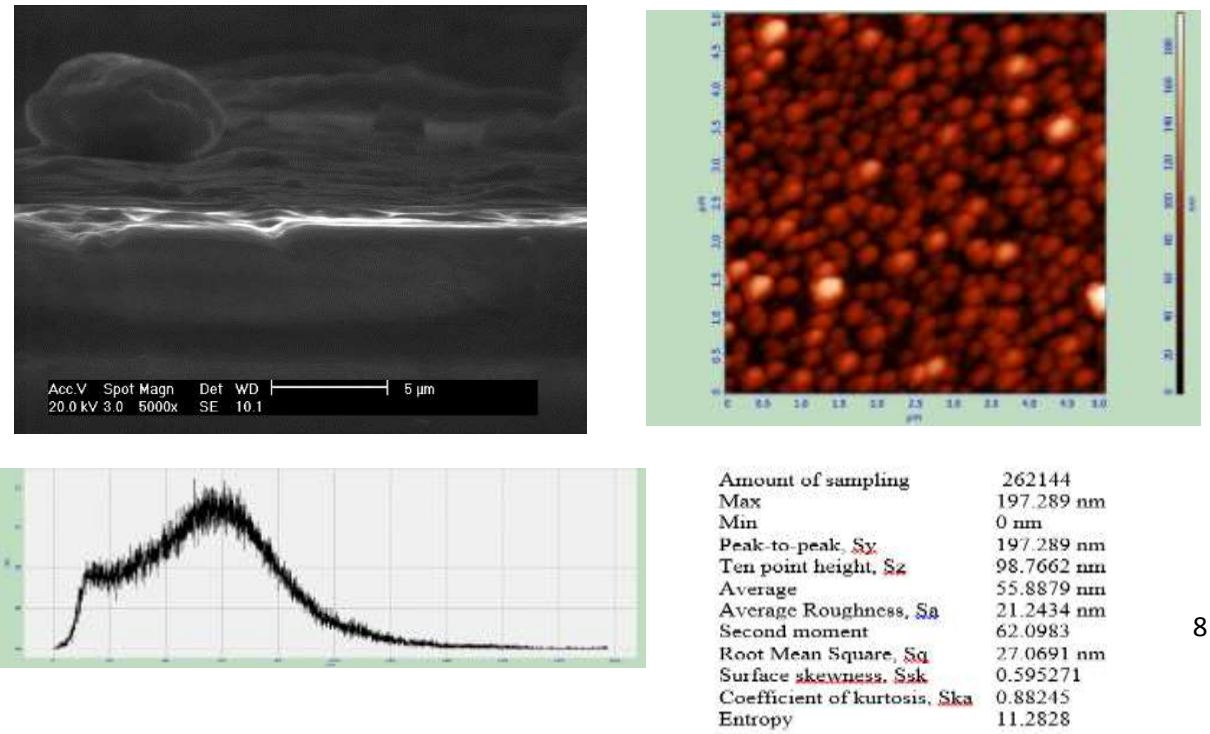

Figure 7. SEM cross-sectional images at 5000x magnification with its AFM image and statistics

SEM cross-section images of 25 layers of Ag/PAA) deposited on glass slides were shown on Figure 7. Deposited polyelectrolytes were seen on the surfaces. AFM statistics show that the deposited nanocomposites has an average height of 55.889 nm, with maximum height of 197.289 nm and average roughness of 21.2434 nm. This shows that even after immobilizing the nanocomposites into L-b-L films, most of the particle sizes remained in the nanoparticles range, which is an essential for the retention of their novel spectroscopic and electronic properties.

Meanwhile, surface analysis of the TiO_2/PAA films generally showed more uniformly sized particles than that of the air-dried solution in mica. Upon formation of layers, the adhered TiO_2/PAA unto the oppositely charged PDDA cannot freely move due to the electrostatic interaction and thus, interconnection and aggregation of the excess PAA chain is not as extensive as compared to the free TiO_2/PAA solution.

(a)

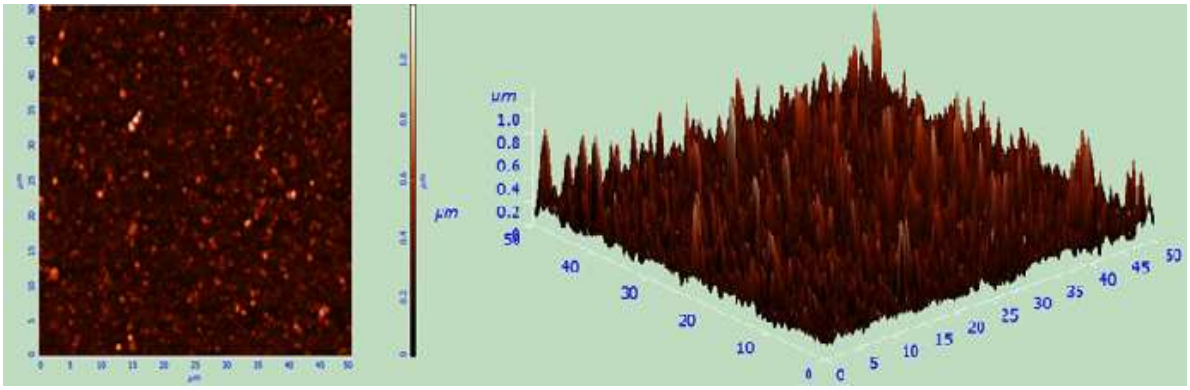

(b)

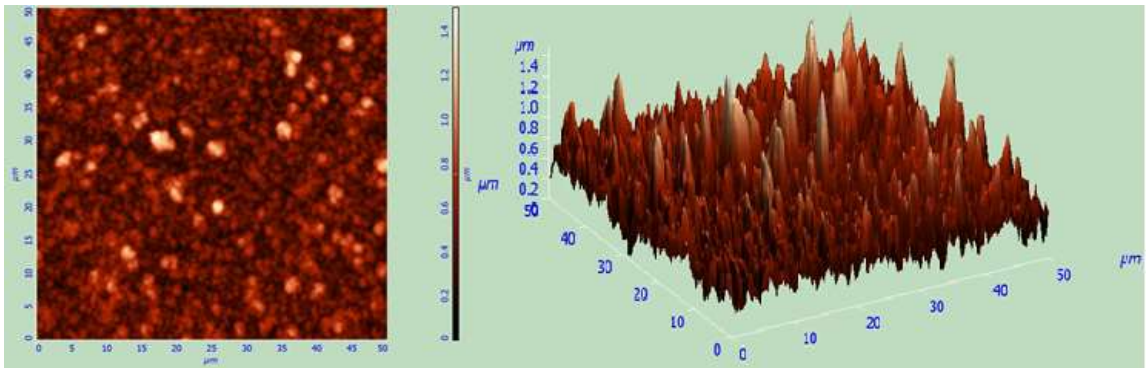

(c)

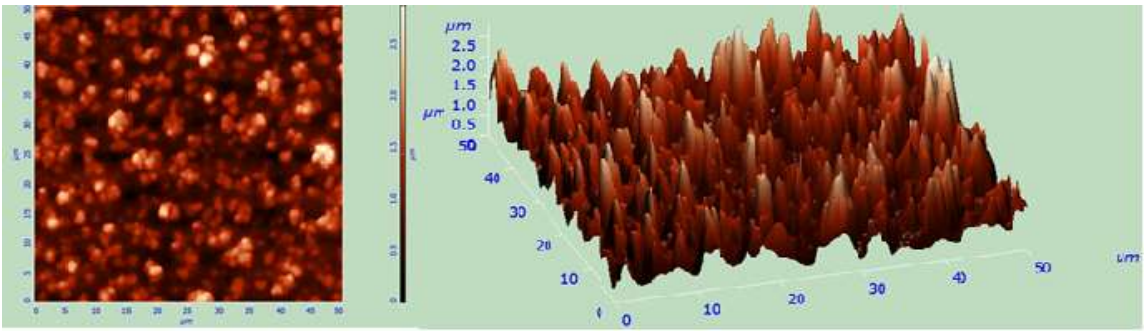

Figure 8. Images of the film formed by LbL deposition of 1:2 TiO_2:PAA solution with PDDA in an area of 50 x 50 μm^2 generated by AFM imaging (left) 2D and (right) 3D for (a) 5 layers, (b) 10 layers and (c) 15 layers

Examination of the height images generated from the three films show that as the number of layers increase, the film roughness decreases. Due to the small number of layer deposit, the 5 layered film has the greatest roughness since film growth is limited to 5 sequences and the distribution of the particles more closely resemble the film. Height image of the film with 5 layers show more pointed peaks and high separation from peak to peak. However, the sizes of the particles are highly deviated. On the other hand, the film with 10 layers, and that of 15 layers showed high-curvature and almost evenly spaced peaks; the latter being better than that of the five layered film. Two-dimensional images of the films shows that the 5-layers have smaller particle sizes and the 10, and 15 layers have larger particle sizes but show more ordered distribution. Sizes of the particles in the 15-layered film showed the lowest deviation from one another as compared to the 5-layered and 10-layered films.

Film thickness

Film thickness was measured by scratching the surface of multi-layer film using the tip of a disposable needle (Terumo) then viewing the scratch portion under AFM. The image of the scratched area was then marked using a white rectangular box where the average cross section can be determined. The average cross section is different from the usual simple linear cross section because the former takes every point in the cross section as average of several points within the selected box. The resulting average values are then designated as the y-axis while the x-axis corresponds to the vertical position of the image. Averaging is important because neither the film surface nor the scraped region is perfectly flat. High ridges can be seen from the graph which resulted from scraping the film. This part should be ignored when measuring thickness. Height was then taken by connecting two points as indicated by the arrows. The height value corresponds to the calculated distance from the y-axis (DY).

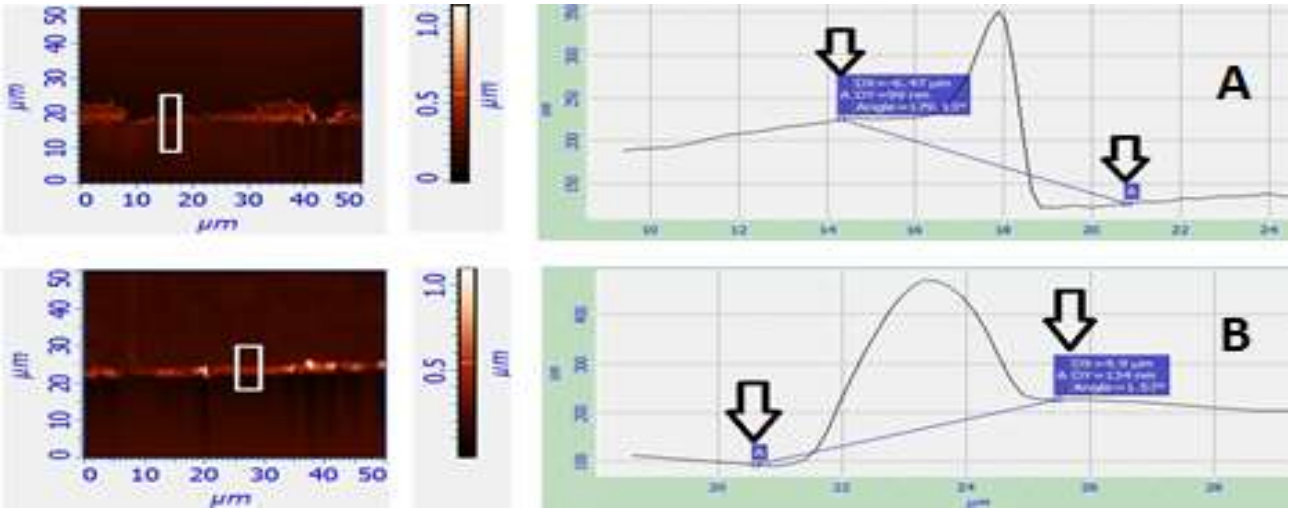

Figure 9. Images of 50 um x 50 um scan size of scratched surface of 25 layers PDDA/Ag/PAA on glass slide (A) and quartz slide (B) with corresponding AFM average cross sectional plot. Film thicknesses (DY) were 99 nm (A) and 134 nm (B)

AFM scans show that the film was successfully removed from the substrates. However, drags of the sample can be noticed as contact mode scan proceeds. Film thickness profile for quartz slides was higher than those of glass slides with respect to the same molecular weights. The mechanism of deposition on the surface of quartz slide could therefore be different with the surface of glass slide. Adsorption of positively-charged PDDA on the negatively-charged surface of quartz could be in an ordered fashion compared with that of an ordinary glass slide, whose surface profile was disordered as seen from the AFM images of clean bare slides in Figure 9. Stacking would therefore result in uniform layering and an increased in thickness for quartz slide.

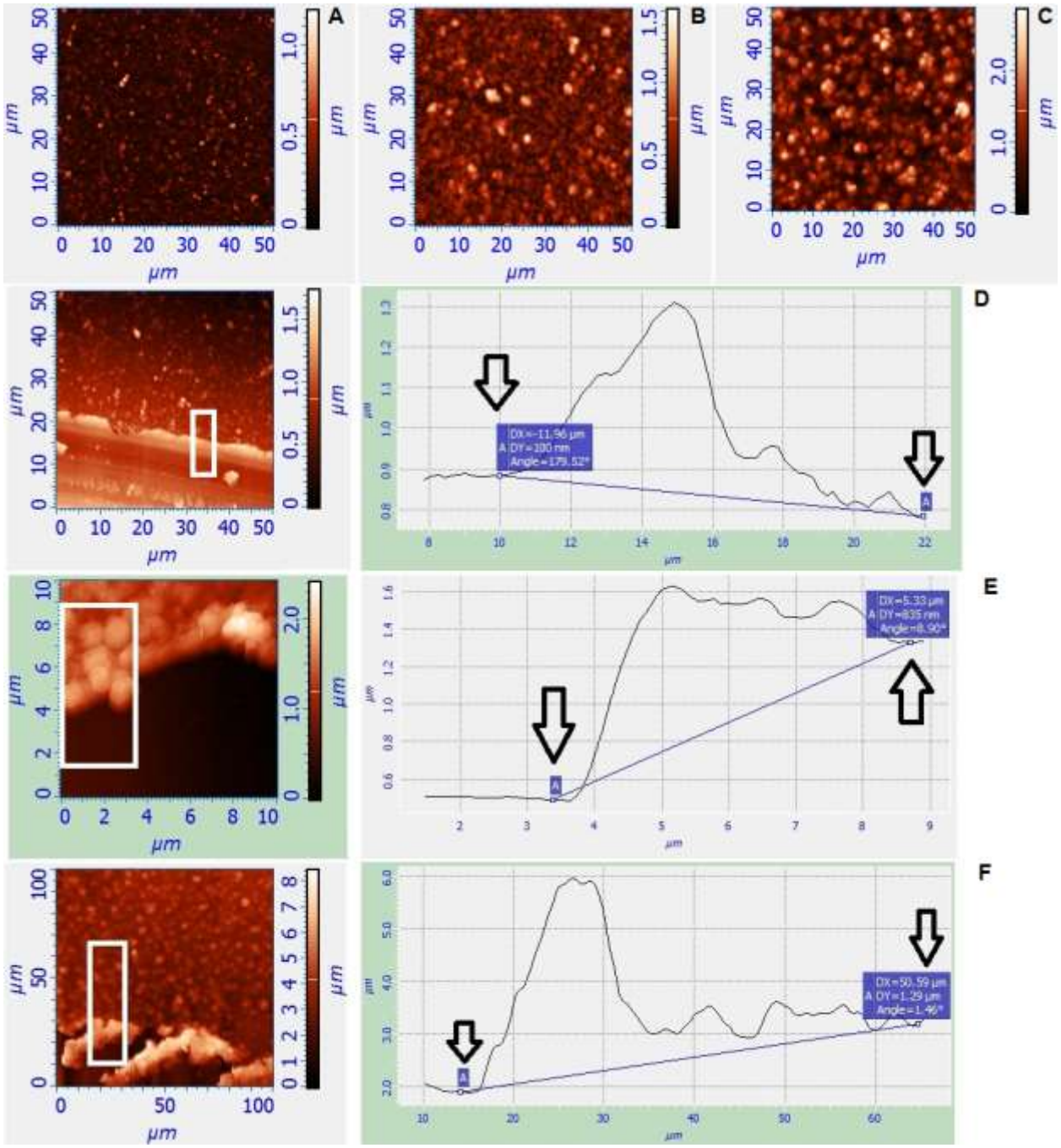

Figure 10. Surface images before scratching the surface of $(PDDA:TiO_2PAA)_n$ on glass slide (450 kDa PAA): n = 5 (A), 10 (B) and 15 (C). Height profiles for 5 (D), 10 (E) and 15 (F) layers after scratching the surface.

Average height was calculated to be 100 nm, 835 nm and 1.29 µm for the films of 5, 10 and 15 layers, respectively, as shown in Figure 10. This increase in thickness can be explained by the charge of the surface of the film in the LbL deposition. In theory, the glass substrate has a negative surface charge; however, ambient air contains positively charge groups that may have adsorbed unto the glass surface lowering its surface charge and consequently, its attraction to the

PDDA monolayer. On the other hand, adsorption of TiO_2PAA unto the film is dependent on the positive surface charge imparted by the PDDA monolayer. An incomplete coating of the film with PDDA will decrease the amount of TiO_2PAA adsorbed due to the repulsion between the substrate and the TiO_2PAA composites. However, as the number of consequent layers are formed, the adsorption of the PDDA and the TiO_2PAA with their respective depositing layer increases since the problem of repulsion with the substrate and the incomplete coating of the previous layer diminishes resulting in an increase in the average thickness of the

Electronic properties of the nanocomposites

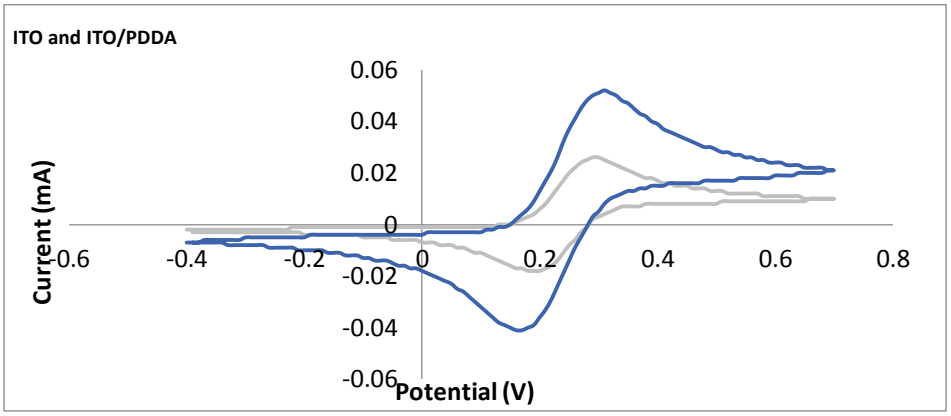

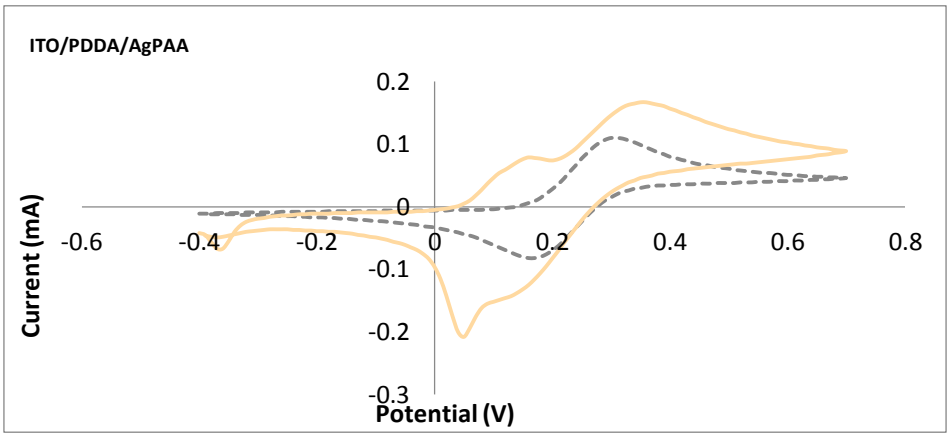

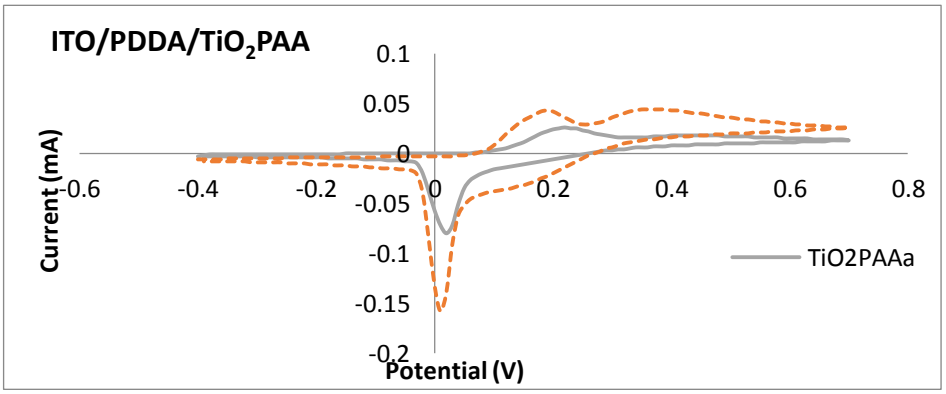

Figure 11: *(Top)* Reversible CV of bare ITO and PDDA on ITO taken on the 3rd cycle. *(Middle)* CV of 5 layers PDDA/Ag/PAA on ITO (dashed = 1st cyle, line = 2nd cycle). *(Bottom)*CV of 5 layers PDDA/TiO_2PAA on ITO (a = 1st cyle, b = 2nd cycle)

Electrochemical measurement of bare ITO-coated glass substrate revealed a quasi-reversible cyclic voltammogram (I_{PC}/I_{PA} = ~1) (Figure 11 *(top)*). The change in peak current (I_{PP}) was 0.027 mA while potential peak separation (ΔE_P) was 0.10 V. This would be the baseline of comparison for characterizing the deposition that occurs on the surface of ITO. The electron transfer rate constant that accounts for the electron transfer resistance is related to changes in peak-to-peak redox current (I_{PP}) and potential peak-to-peak separations (ΔE_P) of voltammograms for various electrode surfaces [16], i.e. polymer deposition on ITO. When ITO was dipped in the solution of polycation PDDA and was checked for its CV, the value of I_{pp} increased to 0.055 mA. ΔE_p also increased to 0.15 V. This is due to the increase in interfacial concentration of hexacyanoferrate anionic probe. The probe had strong affinity towards polycationic layer since the amino groups of PDDA are protonated ($-NH_3^+$).
The first cycle for 5 layers of Ag/PAA/PDDA on ITO shown in Figure 11 *(middle)* revealed an increase in I_{PP} while ΔE_P had almost the same values when compared with PDDA layered on ITO. The slight deviation on ΔE_P is due to the minimal repulsion of the probe with some carboxyl ions ($-COO^-$) outside the surface of nanocomposites. Drastic changes occurred in CV while applying potential on the surface of ITO. This can be seen in the second cycles of PDDA/Ag/PAA on ITO. McAloney et al. [14] presented in their AFM study of multilayer film that there is competitive binding of free salt with the deposited polyelectrolyte on glass slides. Salt ions can penetrate the film, freeing up the polymer segments and allowing to reform with different polymer segments. This forms new lower energy local configurations. The contact is temporary but enough to enhance the mobility within the film. Current that was made to pass within the solution resulted to the appearance of a small peak before the peak that corresponds to oxidation of ferrocyanide to ferriccyanide ion. This anodic peak is attributed to the oxidation of Ag particle forming silver cation. The supporting electrolyte turned into a brownish color after each run.

The same conclusion can be deduced with the voltammogram of PDDA/TiO_2PAA on ITO (Figure 11 *(bottom)*). There were appearances of two peaks. Since salt ions may have penetrated the film, the basicity of the supporting electrolyte hastens the conversion of the surface of TiO_2 from $TiOH_2^+$ to either TiO^- or TiOH with the release of electron manifested in the appearance of small anodic peak current. Meanwhile, large increased in peak current can be seen during cathodic scan. This is due to the lesser repulsion of reducible specie of ferriccyanide with carboxyl group since titania is no longer encapsulated by PAA.

Conclusion

Polymer-encapsulated silver were generated by γ-irradiation of aqueous solutions of $AgNO_3$ in the presence of poly(acrylic acid) as stabilizer and 2-propanol as radical scavenger. The effects of varying the metal-to-polymer ratio on the plasmon bands of Ag/PAA nanocomposite solutions were assessed along with the optical and electronic properties of the immobilized Ag/PAA and nanocomposites. For the case of TiO_2/PAA, the ratio of PAA and TiO_2 present in solution greatly affects the size and distribution of the nanocomposites formed. Excess PAA

interconnect with one another and form thread-like particulates. On the other hand, excess TiO_2 becomes surface for nanocomposite adsorption. The ratio 1:2 TiO_2:PAA formed particulates that has the best particle distribution and particle sizes. Nanoparticle immobilization was done on different silica surfaces via layer-by-layer technique wherein the driving force for thin film formation is due to the electrostatic attraction between the negatively charged polymer shell and positive PDDA molecules. The retention of the plasmon resonance property after immobilization could serve as a probe information of layers. Height profiles and surface morphology can be monitored by spectral and AFM scans.

Acknowledgements
The authors wish to thank Natural Sciences Research Institute (NSRI) for funding the project (Code: CHE-13-2-04) and the Philippine Nuclear Research Institute for γ irradiation of samples.

References
[1] G. Decher, J.D.Hong, J. Scmitt, Buildup of ultrathin multilayer films by self-assembly process: III. Consecutively alternating adsorption of anionic and cationic polyelectrolytes on charged surfaces. Thin Solid Films 210/211 (1992) 831-835.
[2] H. S. Zhou, I. Honma, H. Komiyama, Controlled synthesis and quantum-size effect in gold-coated nanoparticles. Phys. Rev. B 50 (1994) 12052-12056.
[3] S. Zhou, T. Wada, H. Sasabe, Synthesis of nanometer-size silver coated polymerized diacetylene composite particles. J. Chem. Soc., Chem. Commun. (1995) 1525.

[4] M. Steigerwald, L. Brus, Semiconductor Crytallites: A Class of Large Molecules. Acc. Chem. Res. 23 (1990) 183.
[5] L. Peyser, A. Vinson, A. Bartko, R. Dickson, Photoactivated Fluorescence from Individual Silver Nanoclusters. Science 291 (2001) 103-106.
[6] K. L. Kelly, K. Yamashita, Nanostructure of Silver Metal Produced Photocatalytically in TiO2 Films and the Mechanism of the Resulting Photochromic Behavior. J. Phys. Chem. B 110 (2006) 7743-7749.
[7] J. M. Tam, J. O. Tam, A. Murthy, D. Ingram, L. L. Ma, K. Travis, K. Johnston, K. Sokolov, Controlled Assembly of Biodegradable Plasmonic Nanoclusters for Near-Infrared Imaging and Therapeutic Applications ACS Nano. 4 (2010) 2178–2184.

[8] N.Makarava, A.Parfenov, I. Baskakov, Water-Soluble Hybrid Nanoclusters with Extra Bright and Photostable Emissions: A New Tool for Biological Imaging Biophysical Journal 89 (2005) 572–580.
[9] M. Rycenga, C. M. Cobley, J. Zeng, W. Li, C. H. Moran, Q. Zhang, D. Qin, Y. Xia, Controlling the Synthesis and Assembly of Silver Nanostructures for Plasmonic Applications. Chem. Rev. 111 (2011) 3669–3712.
[10] G. Mie, Ann. Phys. 25 (1908) 377.

[11] M. Faraday, Philosophical Transactions of the Royal Society, London, 1857.

[12] M. Treguer, F. Rocco, G. Lelong, A.L. Nestour, T. Cardinal, A. Maali, B. Lounis, Solid State Sci. 7 (2005) 812-818.

[13] J. Belloni, M. Mostafavi, H. Remita, J.-L. Marignier, M.-O. Delcourt, Radiation Induced Synthesis of Mono- and Multi-metallic Clusters and Nanocolloids. New J. Chem. (1998) 1239-1255.
[14] R. A. *McAloney*, M. Sinyor, V. Dudnik, M. C. *Goh*, Atomic force microscopy studies of salt effects on polyelectrolyte multilayer film morphology. Langmuir. 17 (2001) 6655-6663.
[15] S. Liufu, H. Xiao, Y. Li, Adsorption of poly (acrylic acid) onto the surface of titanium dioxide and the colloidal stability of aqueous suspension. Journal of Colloid and Interface Science. 281 (2005) 155-163.
[16] Rajesh, V. Sharma, S. Mishra, A. Biradar, Synthesis and electrochemical characterization of myoglobin-antibody protein immobilized self-assembled gold nanoparticles on ITO-glass plate. Materials Chemistry and Physics. 132 (2012) 22-28.
[17] dela Santa, A. (2002) Novel Polymer Spheres and Nanocomposites from the Collapse of Polyacrylic Acid. National Library of Canada. AMICUS no. 26189629.